NONLINEAR ISSUES ON THE NUMERICAL SIMULATIONS OF THE 9 METER DROP TEST OF A TRANSPORTATION PACKAGE

Miguel Mattar Neto
Carlos Alexandre de Jesus Miranda
Gerson Fainer
mmattar@ipen.br
cmiranda@ipen.br
gfainer@ipen.br
Nuclear and Energy Research Institute, IPEN – CNEN/SP
Av. Prof. Lineu Prestes 2242, 05508-000, São Paulo – SP – Brazil

Abstract. *The requirements for the qualification of transportation packages for nuclear research reactors spent fuel elements are very severe. They include, as a hypothetical accident condition, a 9 meter package free drop on a rigid surface. It is allowed to use shock absorbers made with energy absorbing materials to assure the package functional and structural integrity. To comply with the nuclear safety functions, as the containment of the internal products and biological shielding, the package itself has several components connected to each other in different ways (welded parts, flanged connections, surface contacts, etc.). So, the package structural evaluation under the drop test condition may be conducted by finite element numerical simulations considering several nonlinear aspects as the nonlinear materials models and properties, the different package materials stiffness, and the different types of the interfaces among the package components and between the package and the rigid surface, including the friction in the contacts. This paper presents a discussion on these nonlinear issues based on the numerical simulations of the drop test developed in the design of a package for nuclear research reactors spent fuel elements using ANSYS LS-DYNA code. Comments and conclusions are addressed based on the obtained results.*

Keywords: *Transportation package, Shock absorber, Nonlinearity, Impact, Contact*

1. INTRODUCTION

The radioactive materials transportation is regulated by guides and standards like IAEA (2005) and CNEN (1988). The main purpose of these regulations is to protect persons, property and the environment from the effects of radiation during the transport of radioactive material. This protection is achieved by requiring the containment of the radioactive contents, the control of external radiation levels, the prevention of criticality, and the prevention of damage caused by heat.

The packages for the transportation of nuclear research reactors spent fuel elements are classified as type B due the nature of the radioactive content. The applied qualification requirements in this case are very severe including the so-called normal conditions of transport and the hypothetical accident conditions. These conditions are defined in the regulations (IAEA, 2005 and CNEN, 1988) and it must be demonstrated that the package has to be sturdy enough to resist, among others:

- a drop onto a rigid target so as to suffer maximum damage, and the height of the drop measured from the lowest point of the cask to the upper surface of the target shall be 9 m;
- a puncture resultant from drop so as to suffer maximum damage onto a bar rigidly mounted perpendicularly on a rigid target. The height of the drop measured from the intended point of impact of the cask to the upper surface of the bar shall be 1 m. The bar shall be of solid mild steel of circular section, 15.0 ± 0.5 cm in diameter and 20 cm long unless a longer bar would cause greater damage, in which case a bar of sufficient length to cause maximum damage shall be used. The upper end of the bar shall be flat and horizontal with its edge rounded off to a radius of not more than 6 mm;
- a fire resulting in a temperature of 800 °C for 30 min;
- a submersion to a 200 m depth of water.

The use of shock absorbers is allowed to assure that the resultant deceleration levels in the radioactive content (spent fuel elements) are low enough and to keep the containment functional and structural integrity in the free drop conditions. The shock absorbers are sacrifice devices that must absorb the package kinetic energy in the impact after the drop by means of their deformation. Several materials may be used to fill the shock absorbers such as natural wood, wood composites, low density concretes, metallic foams, polymeric foams, and metallic honeycombs.

The 9 m drop tests are the most critical hypothetical accident conditions. The package qualification under these conditions shall be conducted using full scale models (prototypes), small scale models, numerical simulations and a combination of physical tests and numerical simulations. The choice of the qualification approach depends on economical and safety aspects.

To comply with the nuclear safety functions, as the containment of the internal products and biological shielding, the package itself has several components connected to each other in different ways (welded parts, flanged connections, surface contacts, etc.). So, the package structural evaluation under the drop test conditions should be conducted by finite element numerical simulations using explicit methods and considering several nonlinear aspects as the nonlinear materials models and properties, the different package materials stiffness, and the different types of the contacts between the package components and between the package and the rigid surface, including the friction in the contacts.

This paper presents a discussion on the non-linear aspects (contacts mainly) and the numerical simulations of the 9 m free drops over a rigid surface of half scale model of a transportation package for nuclear research reactors spent fuel elements under different

orientations using a finite element explicit code. A discussion on these nonlinear issues based on these numerical simulations of the drop tests is also assessed and comments and conclusions are addressed based on the obtained results.

2. THE HALF SCALE MODEL OF THE PACKAGE

Figure 1 shows a cross section of the package half scale model under construction to be tested in the near future. Its main parts are: Internal Basket to accommodate the spent fuel elements, one internal and one external stainless steel cylinder connected by two flanges (internal and external) with lead located between the lateral and lower parts, an upper closure (Primary lid) constituted by a shell surrounding a plate of lead, located on the internal flange. The lead constitutes the biological shield against the radiation. There is, also, a plate connected to the external flange by bolts to fix the upper closure (Secondary lid).

There are two shock absorbers, each one surrounded by a thin stainless steel shell. They are connected by four round bars, and are constituted by Oriented Strand Board (OSB) glued plates. Usually, the OSB, a kind of composite or reconstituted wood, has an orthotropic behavior but when confined, as in this project, it behaves as an isotropic material (see next sections).

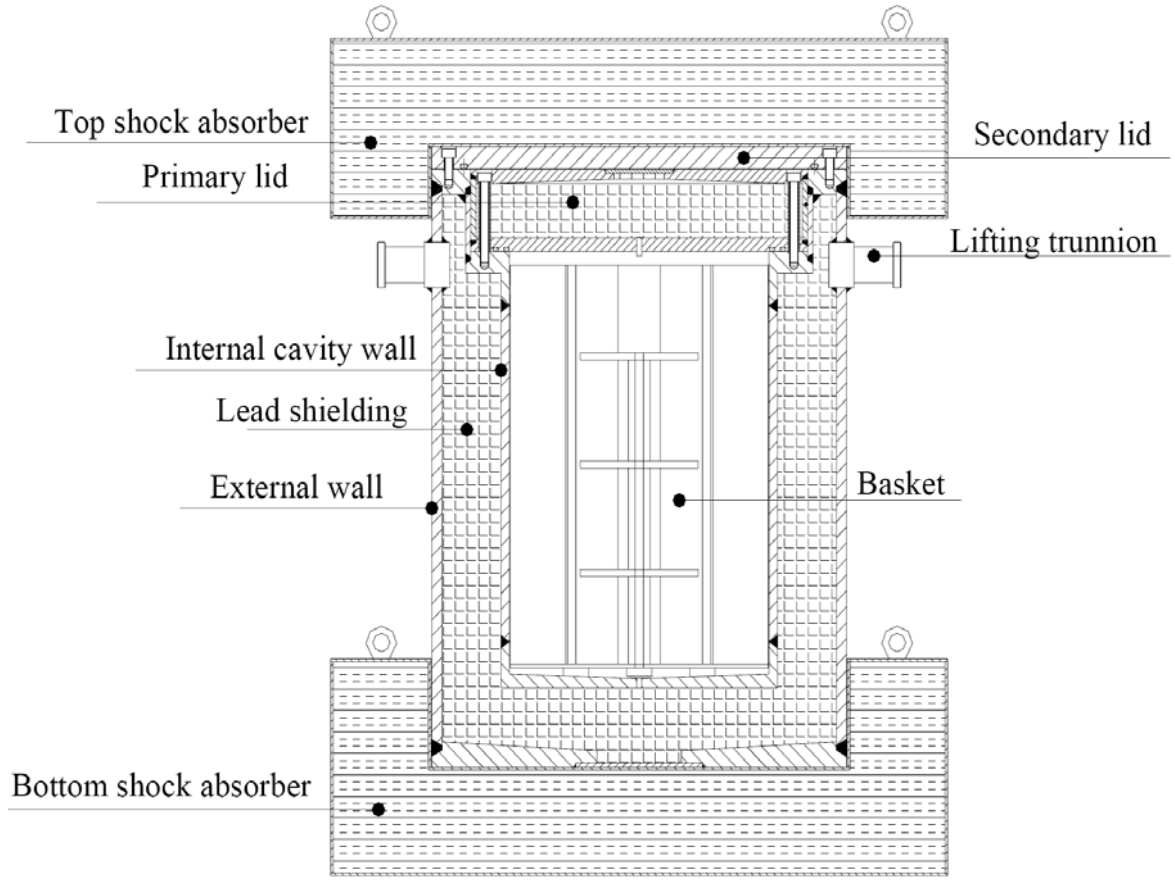

Figure 1- Cross section of the half scale model of the package.

The external cylinder has a diameter of ≈0.50m and it is ≈0.60m high. With the shock absorbers the package overall dimensions are: external diameter ≈0.90m and ≈1.00m high.

Figures 2 and 3 show, respectively, an internal view of the half scale model of the package and the bottom shock absorber partially assembled.

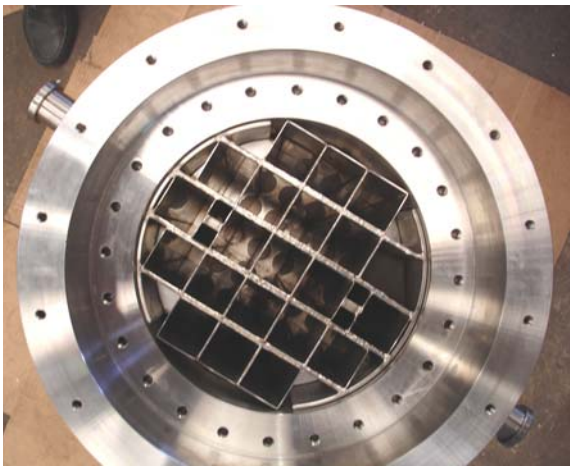

Figure 2- Internal view of the package half scale model.

Figure 3- Bottom shock absorber partial assembling.

3. SHOCK ABSORBERS MATERIAL CHARACTERIZATION

As the properties of the OSB are not well known, especially its response to dynamic loads, a testing campaign was conducted to determine the parameters of interest for the intended use. This material is an engineered, mat-formed panel product made of strands, flakes or wafers sliced from small diameter, round wood logs and bonded with a binder under heat and pressure.

To study the effect of the lateral constraint in the dynamic response of the OSB, both encased and non encased specimens were submitted to impact tests (Mourão, 2007). The specimens, also made of glued layers of OSB, consisted of cylinders with 60 mm in diameter and 30 mm height. The direction normal to the glued surfaces was defined as the specimen perpendicular direction, whereas the glued surfaces define the specimen parallel directions. Besides the perpendicular and parallel directions, the specimens were also tested at 45° angle. The encased specimens were surrounded by a 0.5 mm thick metallic shell.

The averaged stress-strain curves obtained are shown in Fig. 4 (all curves were filtered at 500 Hz, low pass filter) (Mourão, 2007). As can be seen, from Fig. 4, the non encased specimens respond as an anisotropic material. On the other hand, the OSB behaves as a nearly isotropic material when tested under lateral constraint condition.

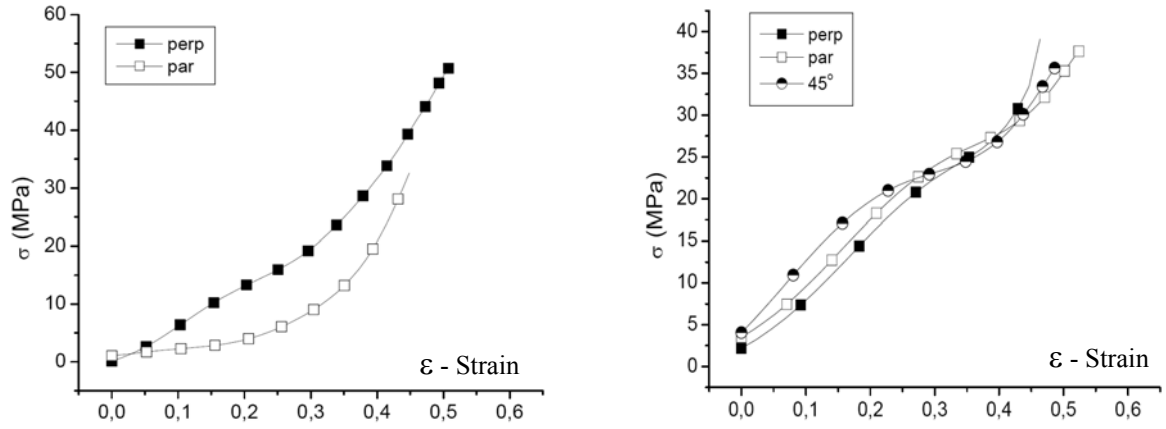

Non-encased specimens

Encased specimens

Figure 4- Shock absorbers material stress-strain curves for different directions.

This behavior can also be seen clearly in Table 1, which shows the values for specific energy U absorbed at 0.45 of strain. The difference in U values in parallel and perpendicular directions for the unconstrained situation is 47% (7.0 to 3.7 MJ/m^3), while the average difference for the encased specimens between the three test directions is less than 10%.

Table 1. Specific energy absorbed (U) @ ε = 0.45

		U (MJ/m^3)
Non-encased specimens	Perpendicular	7.0
	Parallel	3.7
Encased specimens	Perpendicular	7.5
	Parallel	8.2
	45º	8.4

For the encased specimens, the values of Young modulus determined in the three impact test directions are: E_{perp} = 68 MPa (perpendicular direction), E_{par} = 65 MPa (parallel direction) and E_{45} = 81 MPa (45º angle).

Although having the OSB mechanical properties characterization in two conditions obtained from tests with non encased and encased specimens, the choice for the use of the properties of the later may be justified by three reasons:

- The encased behavior of the OSB is not given only by the surrounding steel shell but also from the self lateral constraining without splintering.
- The deformed configurations of the non encased specimens after the impact tests show splintering in outer parts that are not expected to occur in the shock absorbers.
- According to Diersch et al. (1994), only a minor increase in the compression forces can be observed due to the influence of the steel casing with thicknesses of 0,5 mm in wood specimens of diameter of 100 mm, avoiding the specimens lateral splintering in the impact tests.

4. NUMERICAL SIMULATIONS OF THE PACKAGE HALF SCALE MODEL 9 M DROP TESTS

The half scale model of the package structural evaluation under the drop test condition may be conducted by finite element numerical simulations considering several nonlinear aspects as the nonlinear materials models and properties, the different package materials stiffness, and the different types of the contacts between the package components and between the package and the rigid surface, including the friction in the contacts.

In this paper, the numerical simulations of the 9 m free drops over a rigid surface of half scale model of the described transportation package under different orientations were conducted using a finite element explicit code ANSYS LS-DYNA (ANSYS, 2007).

4.1 Contacts modeling

A contact is defined by identifying (via parts, part sets, segment sets, and/or node sets) what locations are to be checked for potential penetration of a slave node through a master segment. A search for penetrations, using any of a number of different algorithms, is made every time step. In the case of a penalty-based contact, when a penetration is found a force proportional to the penetration depth is applied to resist, and ultimately eliminate, the penetration. Unless otherwise stated, the contacts discussed here are penalty-based contacts as opposed to constraint-based contacts. Rigid bodies may be included in any penalty-based

contact but in order that contact force is realistically distributed, it is recommended that the mesh defining any rigid body be as fine as that of a deformable body.

In high velocity impact analysis, the deformations can be very large and predetermination of where and how contact will take place may be difficult or impossible. For this reason, the automatic contact options are recommended as these contacts are non-oriented, meaning they can detect penetration coming from either side of an element.

Due to the impact condition and due to the geometric features of the half scale package showed in Fig. 1, it was used the so-called AUTOMATIC SURFACE TO SURFACE contact option of the ANSYS LS-DYNA code.

This type of contact is a two way contact allowing for compression loads to be transferred between the slave nodes and the master segments. Tangential loads are also transmitted if relative sliding occurs when contact friction is active. A Coulomb friction formulation is used with an exponential interpolation function to transition from static to dynamic friction. This transition requires that a decay coefficient be defined and that the static friction coefficient be larger than the dynamic friction coefficient. The constraint algorithm is based on the algorithm developed by Taylor & Flanagan (1989). This involves a two-pass symmetric approach and allows for compression loads to be transferred between the slave nodes and the master segments. The definition of the slave surface and master surface is arbitrary since the results will be the same.

Modeling the contact between the OSB material (soft) and other steel package parts (rigid) poses several challenges in impact conditions. This is due to its relatively low stiffness of the first when compared with other structural materials which has an indirect effect on its contact-impact interactions with other materials.

Time-step and contact stiffness. In ANSYS LS-DYNA code the default procedure to compute the time-step and the contact stiffness is based on the maximum value of the Young's Modulus E, the maximum slope from the stress-strain curve (E_{curve}). This default approach is conservative to ensure that the computed time-step is stable for all compressive strains. The default value of the modulus from this approach could either be too small (if E is greater than E_{curve}) or too large (if the E_{curve} is greater than E). ANSYS LS-DYNA allows the overriding of this default logic. Suppose a case where the E_{curve} is 10 MPa and E is 50 MPa. Consequently, the E value of 50 MPa was used in the time-step and contact stiffness calculations which is roughly 0.025% of the modulus of steel (200,000 MPa). This huge disparity in stiffness values between the impacting bodies is naturally going to cause instabilities in contact. The alternative approach is to use a penalty contact using soft-constraint algorithm. However, ANSYS LS-DYNA always uses a penalty based approach based on material stiffness for contact between a rigid body and deformable bodies. Therefore, it is recommended to alter the modulus to a value at least 1% of the modulus of the impacting material (which, is in this case, is steel).

Extended Stress-Strain Curve. An important point in contact modeling of the impact between materials with large differences in their stiffness is the procedure to avoid the collapse of the first row of soft materials, due to large compressive strains, that leads to an abnormal run ending with negative volumes issues. ANSYS LS-DYNA follows strictly the stress-strain curve to the last input stress-strain point. For strain magnitudes larger than the last input point in the curve, the code extrapolates using the last slope. This may yield small stress values and fails to model the bottoming out effect that occurs at large compressive strains. The fix to this is to manually provide an exponentially increasing curve to cover compressive strains to a minimum of 95-99%. It must be noticed that the manual curve must be smooth. The modified curve used in this paper is showed in Fig. 5.

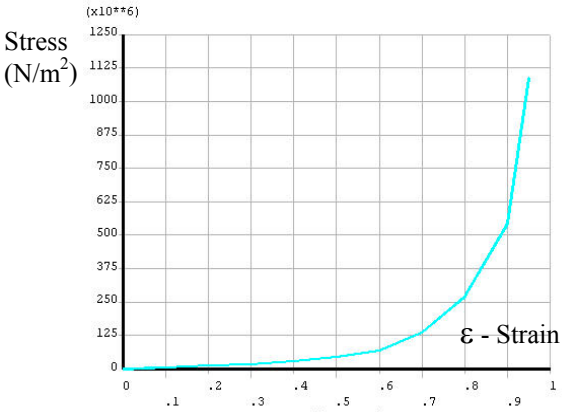

Figure 5- Modified shock absorbers material stress-strain curves used in the analyses.

Increased Solid Element Thickness in Contact. Some penetration between soft and rigid materials can be found during the maximum compressive strain. This may be attributed to the way the segment thickness is computed for solid elements. Much like shell elements, in which the mid-surface is offset in both directions of the segment normal, the solid segments maximum allowable thickness is also computed. The amount of maximum allowable thickness is based on a small percentage (5%) of the solid element diagonal which, based on the element geometry, could be very small making it vulnerable to nodal release. So, it is recommended to increase the offset thickness to a value adequate to ensure that no nodes are released from contact.

4.2 Materials modeling

The half scale package model materials are indicated in Table 2.

Table2. Half scale package model materials

Cask Part	Material
Lower shell	stainless steel
Bottom shock absorber	wood (OSB)
Inner shell	stainless steel
Shielding	lead
Outer shell	stainless steel
Top shock absorber	wood (OSB)
Upper shell	stainless steel
Tie bars	stainless steel

The shock absorbers filling material (OSB) was modeled as crushable foam with its correspondent curve following an isotropic linear behavior until a strain of $\varepsilon = 0.45$, extended until $\varepsilon = 0.95$, as per Fig. 5, to avoid numerical instabilities. The rigid surface was modeled with the ANSYS LS-DYNA RIGID option. The steel parts, including the round bars, as well as the lead ones were modeled as Bilinear Isotropic Material (BISO). The basket was modeled in a simplified way as a continuous mass with fictitious values and a density value 'calibrated' to reproduce the mass predicted to fill de cask. All adopted material properties, except OSB, can be seen in Table 3.

Table 3: Materials properties adopted in the analyses

	Steel	Lead	Mass	Bar	Rigid Surface	units
E - Young's modulus	200e9	14e9	2e9	200e9	200e9	N/m^2
ν - Poisson's ratio	0.30	0.42	0.0	0.30	0.30	---
ρ - Density	7500	11500	600	7500	7500	Kg/m^3
σ_{ys} - Yield stress	310e6	14e6	-----	310e6	-----	N/m^2
E' - Tangent modulus	7.6e8	1.0e7	-----	7.6e8	-----	N/m^2

4.3 Finite element model

A 180° finite element model, showed in Fig. 6, was developed using solid and shell elements and considering the symmetries in the structures. Parts as trunnions, bolts and threads were not modeled. This model can be rotated to cover all drop orientations that must be simulated (see Fig. 6). As said before, automatic surface to surface contacts were considered in all interfaces between different parts.

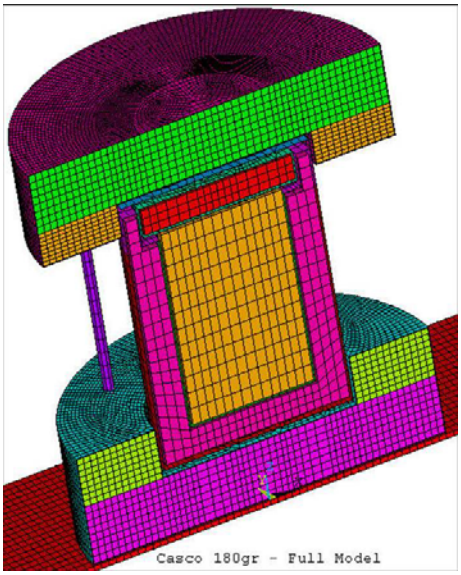

Front view

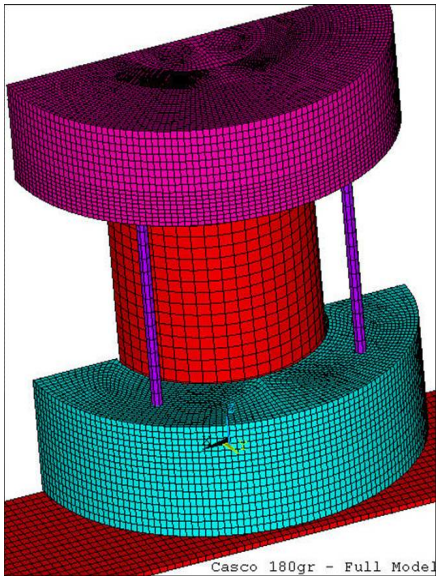

Back view

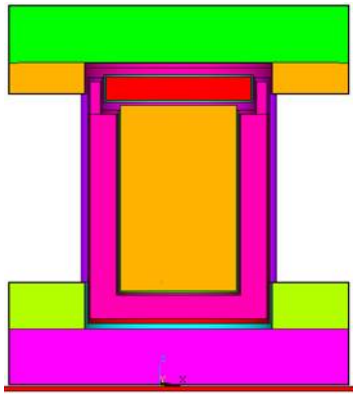

Vertical orientation (0°)

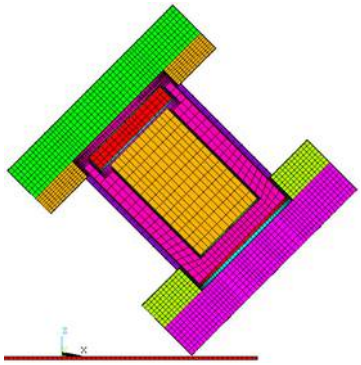

Inclined orientation (45°)

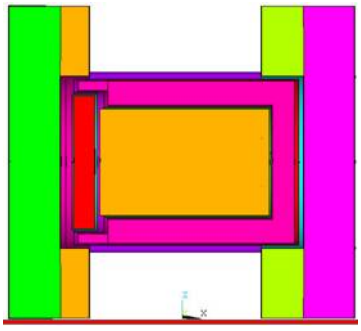

Horizontal orientation (90°)

Figure 6- 180° finite element model and drop orientations.

4.4 Numerical simulations

The analysis starts as the model touches the rigid surface, so the applied initial velocity (13.3 m/s) corresponds to the 9m free drop. Additionally the gravity acceleration was applied to the model.

Three analyses were performed simulating the vertical, the side (horizontal) and the 45° (corner) impact. In general, the results in terms of displacements along the time are smooth while in terms of accelerations a filter like Butterworth-type should be adopted due to the noise introduced by the successive integrations.

5. RESULTS

The main results of the numerical simulations presented in this paper are related to the displacements, velocities and accelerations of some chosen points, the comparison between the contact modeling issues already discussed and the deformed shape of the structures in the time of their maximum deformation.

The first results to be showed, Fig. 7, are the curves displacement versus time, velocity versus time and acceleration versus time of the finite element central node for the horizontal 9 m drop test (as mentioned before, to the latter should be applied a Butterworth-type filter).

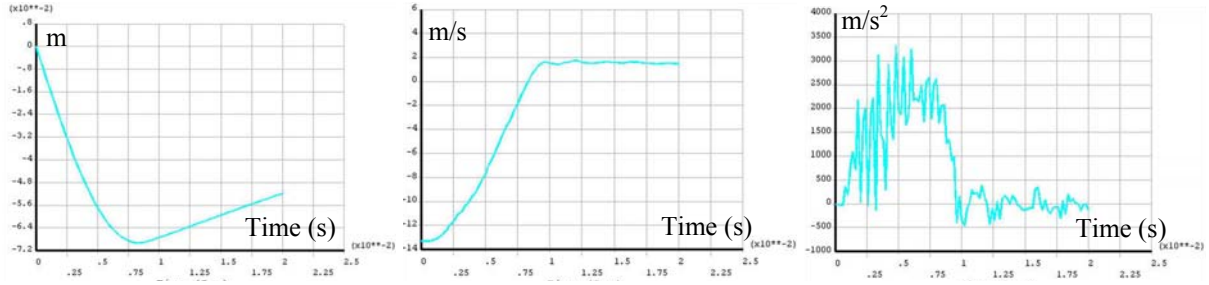

(a) Displacement X time (b) Velocity X time (c) Acceleration X time

Figure 7- Movement curves of the 180° finite element model central node.

The next results are those related to the comparison between the contact modeling issues. Figures 8 and 9 show two deformed shapes in two different conditions for the corner drop simulations. In Fig. 8, the contact modeling does not include the improvements discussed in section 4.1 above related to time-step and contact stiffness and increased solid element thickness in contact while in Fig. 9 all improvements were included in the contact modeling.

At the beginning, some numerical experiments were also conducted varying the static and dynamic friction coefficients in the contacts.

No special results were obtained and the usual coefficient values of 0.15 for static friction and 0.09 for dynamic friction were used in the remaining analyses.

Figure 10 shows some aspects of the deformed configurations for the three impact directions already analyzed at the moment of their maximum deformation: vertical, side or horizontal and corner impact (45°). Figure 10.b shows only the “lower” limiter once the “upper” one has an almost identical behavior (they don’t behave identically because their projects are slightly different – their maximum individual deformations are, respectively, 66.1mm and 69.1mm). Also, in the vertical and side impact figures one can see the almost uniform deformation in the limiter impact under and due to the external cylinder. This viewing is allowed by the dark lines representing the (initial) non deformed situation.

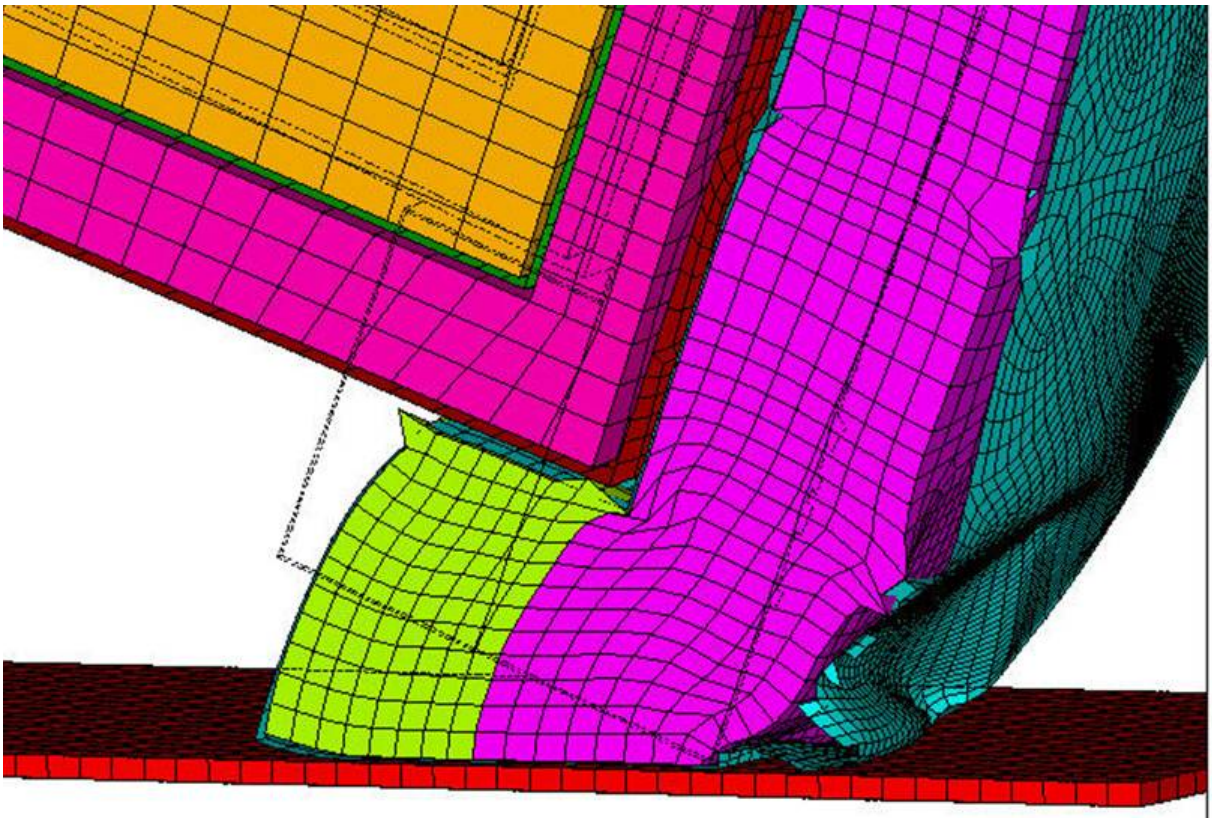

Figure 8- 180° finite element model deformed shape without improved contact modeling.

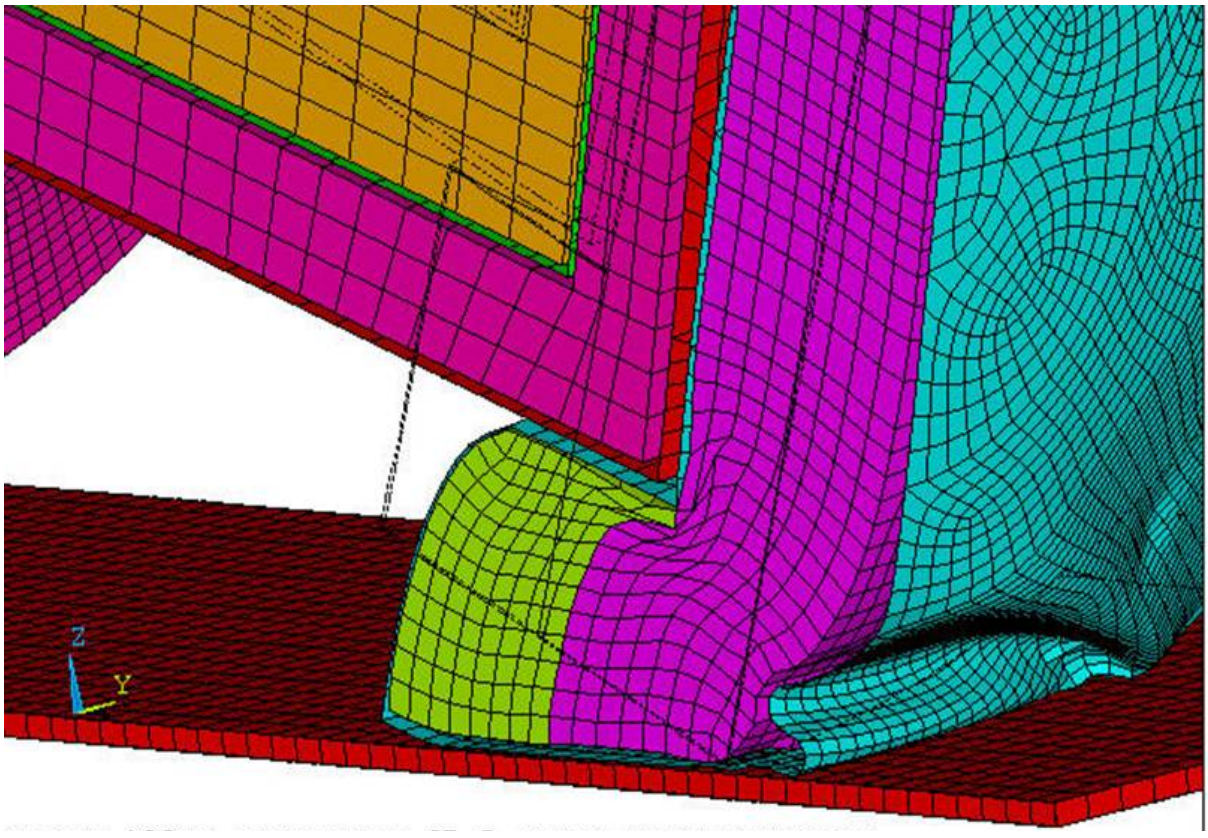

Figure 9- 180° finite element model deformed shape with improved contact modeling.

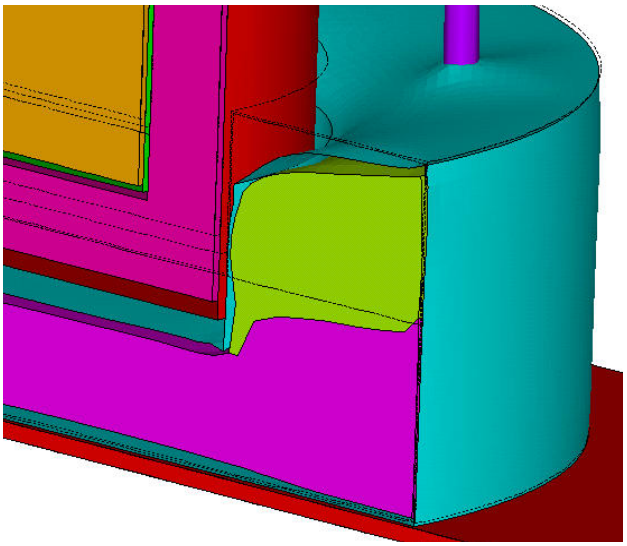

(a) Vertical drop

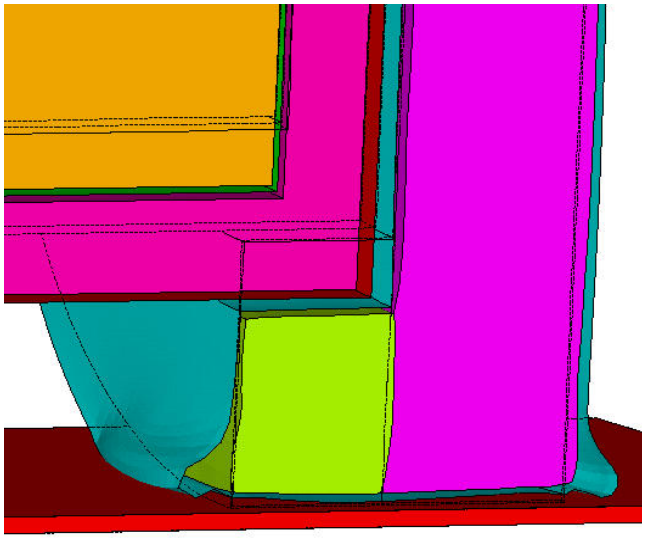

(b) Horizontal or Side drop

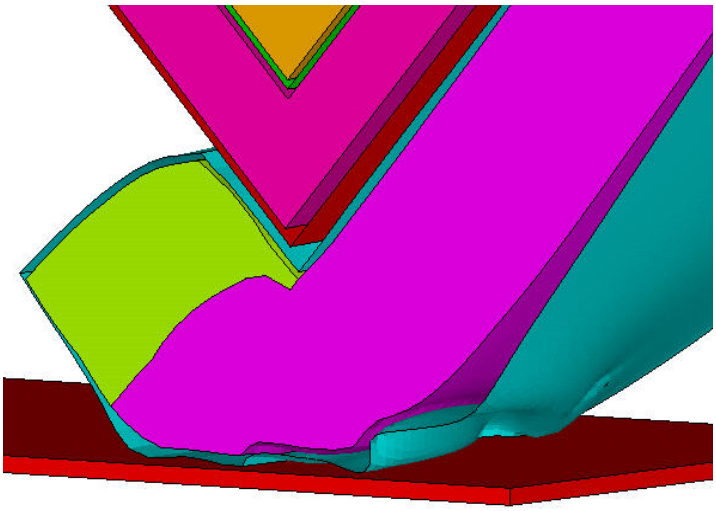

(c) Corner drop

Figure 10- Final deformed shapes for three impact orientations.

Some important results for the package project are those related to maximum decelerations and deformations. Table 4 presents some of the obtained results in terms of the package maximum deceleration (after a filtering operation) and deformation in the shock absorbers.

Table 4: Main results from numerical simulations

	Deceleration (g)	**Deformation (mm)**
Vertical orientation	430	45.5
Horizontal orientation	250	67.6
Corner (45°) orientation	130	153.6

g – gravity acceleration

6. COMMENTS AND CONCLUSIONS

The obtained results have shown an expected behavior, especially the deformed configuration at the moment of their maximum deformation. In particular, the smoothness of the deformed shock absorber shell in Fig. 9 shows the goodness of the meshing level adopted in the shock absorbers. Also, the comparison of the Fig. 8 and 9 shows the good behavior of the model with the defined contact parameters overriding the problems discussed in the text.

Figure 7 shows the need of a filtering procedure to obtain the maximum acceleration in a given point of interest. Table 4 shows the maximum deceleration and deformation values for three drop orientation. Preliminarily, one can say the vertical drop is the worst situation once it produces 430 g deceleration in the internal (dummy) mass. These values can be directly compared with the ones to be measured in the test campaign to be performed in the near future.

However, to apply these deceleration values, experimentally measured or numerically calculated when using scaled models instead of full scale model, a correction factor should be applied to take into account the scale, shown in Shappert (1998). In this case, 1:2 scale, the measured or the calculated deceleration should be divided by two to compare with or to predict results to full scale model. So, a maximum value of 215g should be expected for the prototype (full scale) which is compatible with the expected strength of the package internals.

REFERENCES

ANSYS LS-DYNA 2007. ANSYS Mechanical and LS-DYNA 11.0 Release, Canonsburg, ANSYS Inc., PA, USA.

CNEN, 1988. Transporte de Materiais Radioativos, Comissão Nacional de Energia Nuclear, Rio de Janeiro, RJ (CNEN-NE-5.01). (in Portuguese)

Diersch, R., Weiss, M. & Dreier, G., 1994. Investigation of the impact behaviour of wooden shock absorbers, Nuclear Engineering and Design, V. 150, p. 341-348.

IAEA, 2005. Regulations for the Safe Transport of Radioactive Material, 2005 Edition, Safety Requirements No. TS-R-1, Vienna, Austria.

Mourão, R. P., 2007. Characterization of Shock Absorbing Materials for Packages, Proceeding of the 2007 International Nuclear Atlantic Conference – INAC 2007, CD-ROM, Santos, SP, Brazil, paper R13-1240, 7 p.

Shappert, L. B. (ed.), 1998. THE RADIOACTIVE MATERIALS PACKAGING HANDBOOK Design, Operations, and Maintenance, ORNL Report ORNL/M-5003, USA.

Taylor, L. M. & Flanagan, D. P., 1989. PRONTO3D A three dimensional transient solid dynamics program, SANDIA Report SAND87-1912, NM, USA.